Hydrologic sensitivity of the Kharaa river discharge in Mongolia

Yo. Amarbayasgalan[1], T. Hiyama[2], T. Sayama[3], A. Dashtseren[1], Ya. Jambaljav[1]

[1] *Institute of Geography and Geo-ecology, Mongolian Academia of Sciences, Mongolia*
[2]*Institute for Space-Earth Environmental Research, Nagoya University, Japan*
[3] *Disaster Prevention Research Institute, Kyoto University, Uji, Japan*

Abstract

The purpose of this study is to investigate long term runoff trends of the Kharaa river discharge in Mongolia. In the estimation of river runoff, we have applied two different hydrological models (RRI and HBV models). These models have been applied using a 10-years data set, which was split into two durations for calibration and validation. We used three statistical variables including Nash-Sutcliffe efficiency (NSE), coefficient of determination (r^2) and relative volume error (VE) to evaluate the model performance. The evaluated statistics of RRI model were NSE = 0.80, r^2 =0.89, VE = 0.04 in the calibration period and NSE = 0.89, r^2 = 0.89, VE = 0.01 in the validation period. On the contrary, NSE was 0.5–0.8 for the HBV model. To quantify the hydrologic sensitivity, this study succeeded to simulate long-term rainfall-runoff for the entire river basin (14,530 km^2) using RRI and HBV model.

Keywords: Long term runoff trends Rainfall, Runoff, RRI model, HBV model

Introduction

Near surface air temperature has increased by 2.07 ℃ during the last 70 years in Mongolia. This quite large warming has occurred more intensively in the mountainous regions than in the Gobi and steppe regions of Mongolia (MARCC, 2014). The interannual variations in summer precipitation and atmospheric circulation patterns showed a significant increasing trend in geopotential height in the lower-level of the troposphere since the mid-1980s over Mongolia (Hiyama et al., 2016). Thus, we need to assess impacts of climate change on river discharge in Mongolia. In this study we used a model-based approach and compared the simulated results in the Kharaa river basin, which is one of the most important agricultural regions in Mongolia. One of the advantages of the model-based approach is the ability to evaluate monthly or daily runoff variations. Previously, Rainfall-Runoff-Inundation (RRI) model (Sayama et al., 2015) has been applied mainly in the rivers of South-East Asia. On the contrary, Hydrological Bureau Water balance-section (HBV) model has been applied in more than 40 countries all over the world.

In this study, we applied the RRI model to the Kharaa river basin. The RRI model simulates rainfall-runoff and flood inundation processes on a 2-D basis at a river basin scale. Since these two processes interact with each other, the concept of the RRI model with forced rainfall is regarded to be suitable to estimate the elasticity of runoff and flood inundation (Sayama et al., 2015).

This study especially focuses on investigating long term runoff trends of Kharaa river discharge using the RRI and HBV models. The application of RRI model to the rivers in Mongolia is the first case. Based on the simulation results, we compared statistical results obtained from the two hydrological models, and analyzed the relationship among rainfall and runoff for the entire Kharaa river basin.

Study area

The Kharaa river basin locates in north-central parts of Mongolia. Its drainage area covers 14,530 km^2, and the river length is 291 km. The Kharaa basin is one of the tributaries of the Orkhon river. Upstream sites are located in the sporadic-isolated permafrost zone.

Methods

RRI model Structure Overview

Structure of the RRI model is a two-dimensional (2-D) model capable of simulating rainfall-runoff and inundation simultaneously (Sayama et al., 2012: Figure.1). For better representations of rainfall-runoff-inundation processes, the RRI model simulates also lateral subsurface flow, vertical infiltration flow and surface flow. The lateral subsurface flow, which is typically more important in mountainous regions, is treated in terms of the discharge-hydraulic gradient relationship, which takes into account both saturated subsurface and surface flows. On the other hands, the vertical infiltration flow is estimated by using the Green-Ampt (G-A) model. The flow interaction between the river channel and slope is estimated based on different overflowing formulae, depending on water-level and levee-height conditions.

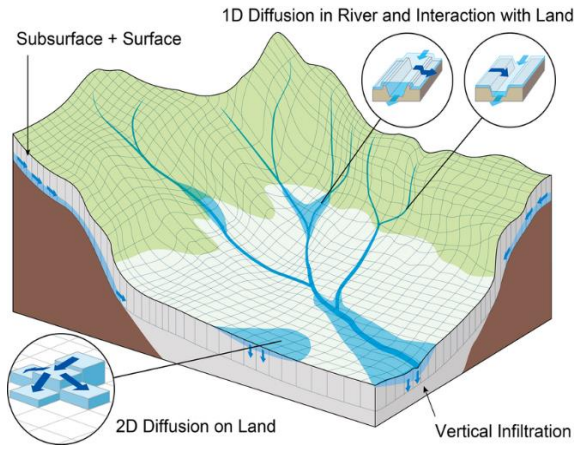

Figure 1. Schematic diagram of the rainfall-runoff-inundation (RRI) model (Sayama et al., 2012).

All the land grid cells can receive rainfall and contribute to rainfall-runoff flowing through other land grid cells and river channels. Meanwhile, they are subject to inundation due to multiple causes: overtopping from river channels, expansion of inundation water from surrounding land grid cells, accumulation of local rainwater of any combination of the three. Hence, the RRI model does not structurally distinguish between rainfall-runoff and flood inundation processes; instead, it solves water flow hydrodynamically. In terms of its application to an entire river basin with rainfall input, the model is similar to grid cell-based distributed rainfall-runoff models. While typical rainfall-runoff models fix flow directions at each grid cell based on surface topography, the RRI model changes flow directions dynamically (Sayama et al., 2015).

It is applicable to an entire river basin. It simulates flow interactions between land and river channels with considerations of levees, so that the RRI model does not require a specification an overflowing point and its overtopping discharge, which are typically required as boundary conditions when using inundation models. Another feature of the RRI model is the acceptance of rainfall and potential evapotranspiration as model input.

It estimates actual evapotranspiration based on the soil moisture conditions and simulates surface and subsurface flows, numerically solved by an adaptive time step Runge-Kutta algorithm (Cash and Karp, 1990; Priess et al., 1992), enables the RRI model to run fast and stable calculations, even for a large river basin with mountainous and plain areas.

Governing Equations of RRI model

A method to calculate lateral flows on slope grid-cells is characterized as "a storage cell-based inundation model" (e.g. Hunter et al. 2007). The model equations are derived-based on the following mass balance equation (1) and momentum equation (2) for gradually varied unsteady flow.

$$\frac{\partial h}{\partial h} + \frac{\partial q_x}{\partial x} + \frac{\partial q_y}{\partial y} = r - f \quad (1)$$

$$\frac{\partial q_x}{\partial t} + \frac{\partial u q_x}{\partial x} + \frac{\partial v q_x}{\partial y} = -gh\frac{\partial H}{\partial x} - \frac{\tau_x}{\rho_w} \quad (2)$$

$$\frac{\partial q_y}{\partial t} + \frac{\partial u q_y}{\partial x} + \frac{\partial v q_y}{\partial y} = -gh\frac{\partial H}{\partial y} - \frac{\tau_y}{\rho_w} \quad (3)$$

where, "h" is the height of water from the local surface, "q_x and q_y" are the unit width discharges in x and y directions, "u" and "v" are the flow velocities in x and y directions, "r" is the rainfall intensity, "f" is the infiltration rate, "H" is the height of water from the datum, "ρ_w" is the density of water, "g" is the gravitational acceleration, and "τ_x" and "τ_y" are the shear stresses in x and y directions. The second terms of the right-hand side of (2) and (3) are calculated with the Manning's equation.

$$\frac{\tau_x}{\rho_w} = \frac{gn^2 u\sqrt{u^2+v^2}}{h^{1/3}} \quad (4)$$

$$\frac{\tau_y}{\rho_w} = \frac{gn^2 u\sqrt{u^2+v^2}}{h^{1/3}} \quad (5)$$

where "n" is the Manning's roughness parameter. Under the diffusion wave approximation, inertia terms (the left-hand sides of (2) and (3)) are neglected. The following equations are derived by separating x and y directions (i.e. ignoring v and u terms in equations (2) and (3) respectively),

$$q_x = -\frac{1}{n}h^{\frac{5}{3}}\sqrt{\left|\frac{\partial H}{\partial x}\right|}\,sgn\left(\frac{\partial H}{\partial x}\right) \quad (6)$$

$$q_y = -\frac{1}{n}h^{\frac{5}{3}}\sqrt{\left|\frac{\partial H}{\partial y}\right|}\,sgn\left(\frac{\partial H}{\partial y}\right) \quad (7)$$

where, "sgn" is the signum function. The RRI model spatially discretizes mass balance equation (1) as follows:

$$\frac{dh^{i,j}}{dt} + \frac{q_x^{i,j-1} - q_x^{i,j}}{\Delta x} + \frac{q_y^{i,j-1} - q_y^{i,j}}{\Delta y} = r^{i,j} - f^{i,j} \quad (8)$$

where "$q_x^{i,j}, q_y^{i,j}$" are x and y direction discharges from a grid cell at (i, j).

Water depths and discharges are calculated by combining the equations of (6), (7) and (8) at each grid cell of each time step. One important difference between the RRI model and other models is that the former uses different forms of the discharge-hydraulic gradient relationship, so that it can simulate both surface and subsurface flows with the same algorithm. The RRI model replaces the equations (6) and (7) with the following

equations of (9) and (10), which were originally conceptualized by Ishihara and Takasao (1962) and formulated with a single variable by Takasao and Shiiba (1976, 1988) based on kinematic wave approximations. The first equations in (9) and (10) ($h \leq d_a$) describe the saturated subsurface flow based on the Darcy law, while the second equations ($d_a \leq h$) describe the combination of the saturated subsurface flow and the surface flow. The hydraulic gradient is assumed to be equal to the topographic slope, for the kinematic wave model, whereas the RRI model assumes the water surface slope as the hydraulic gradient.

$$q_x = \begin{cases} -k_a h \frac{\partial H}{\partial_x}, & (h \leq d_a) \\ -\frac{1}{n}(h-d_a)^{5/3}\sqrt{\left|\frac{\partial H}{\partial x}\right|}\, sgn\left(\frac{\partial H}{\partial x}\right) - k_a h \frac{\partial H}{\partial x}, & \end{cases} \quad (9)$$

$$q_y = \begin{cases} -k_a h \frac{\partial H}{\partial_y}, & (h \leq d_a) \\ -\frac{1}{n}(h-d_a)^{5/3}\sqrt{\left|\frac{\partial H}{\partial y}\right|}\, sgn\left(\frac{\partial H}{\partial y}\right) - k_a h \frac{\partial H}{\partial y}, & \end{cases} \quad (10)$$

where "k_a" is the lateral saturated hydraulic conductivity and "d_a" is the soil depth times the effective porosity.

Here we calculate infiltration loss "f" with the Green-Ampt infiltration model (Raws et al., 1992).

$$f = k_v\left[1 + \frac{(\emptyset - \emptyset_i)s_f}{F}\right] \quad (11)$$

where "k_v" is the vertical saturated hydraulic conductivity, "$\emptyset$" is the soil porosity, "ϑ_i" is the initial water volume content, "S_f" is the suction at the vertical wetting front and "F" is the cumulative infiltration depth.

Interactions of water between slope and river

Water exchange between a slope grid cell and an overlying river grid cell was estimated as a function of the relationships between the slope water level, river water level and levee height and ground. River and slope water exchange, the following four different conditions. For each condition, different overtopping formulae are applied to calculate the unit length discharge from slope to river (q_{sr}) or from river to slope (q_{rs}), which are then multiplied by the length of the river vector at each grid cell to calculate the total exchange flow rate (Iwasa and Inoue, 1982).

(a) When the river water level is lower than the ground level, q_{sr} is calculated by the following step fall formula.

$$q_{sr} = \mu_1 h_s \sqrt{g h_s} \quad (12)$$

where "μ_1" is the constant coefficient (= (2/3)), and "h_s" is the water depth on a slope cell. As far as the river water level is lower than the ground level, the same equation is used even for the case with levees so that the slope water can flow into the river.

(b) When the river water level is higher than the ground level and both the river and slope water levels are lower than the levee height, no water exchange is assumed between the slope and river.

(c) When the river water level is higher than the levee crown and the slope water level, the following formula is used to calculate overtopping flow q_{sr} from river to slope.

$$q_{rs} = \begin{cases} \mu_2 h_1 \sqrt{2gh_1} & h_2/h_1 \leq 2/3 \\ \mu_3 h_2 \sqrt{2g(h_1 - h_2)} & h\_2/h\_1 > 2/3 \end{cases} \quad (13)$$

where "μ_2 and μ_3" are the constant coefficient (=0.35, 0.91), and h_1 is the difference between the river water level and the levee crown. "μ_2 and μ_3" are the constant coefficient (=0.35), and "h_1" is the difference between the river water level and the levee crown.

(d) When the slope water level is higher than the levee height and the river water level, the same formula as (2) is used to calculate overtopping flow q_{sr} from slop to river. In this case, "h_1" is the elevation difference between the slope and the river, and "h_2" is the elevation difference between the river and the levee crown.

RRI model application

The RRI model is applied to the entire Kharaa river basin. It was set up using the DEM (digital elevation model). Flow direction and flow accumulation were delineated from Hydro SHEDS 30 s (Lehner et al., 2008) and upscaled to a 60 s (approximately 2 km) resolution (Masutani et al., 2006). The RRI model uses flow direction and accumulation only to determine river channel locations but not for flood routing, since the flow direction varies depending on hydraulic gradients. Local river depths D (m) and widths W (m) were decided, based on cross-section information at the stations and measured site, while for tributaries with no cross-section information, we approximated widths and depths using the following (14) and (15) (Coe et al., 2008).

$$W = C_W A^{S_W} \quad (14)$$

$$D = C_D A^{S_D} \quad (15)$$

where "A" is the upstream contributing area (km^2) and "C_W", "S_W", "C_D," and "S_D" are regression parameters, whose values were estimated from river cross-section data.

The obtained parameters were C_W = 20.0, S_W = 3.50, C_D = 2.0, and S_D =0.18. These equations are capturing the general characteristics of the river's cross sections becoming wider and deeper downstream. To set model parameters, the area was first classified into two areas:

mountains and plains. At this time, we have evaluated runoff of hydrograph and long-term changes variables depending on rainfall.

Model simulation results

We split the duration between 1995 and 2013 into a calibration period (1995-2005) and validation period (2005-2013). Figure 2 compares observed daily discharge with simulated discharge using RRI and HBV models. Both models could reproduce daily river discharge well for both calibration and validation periods.

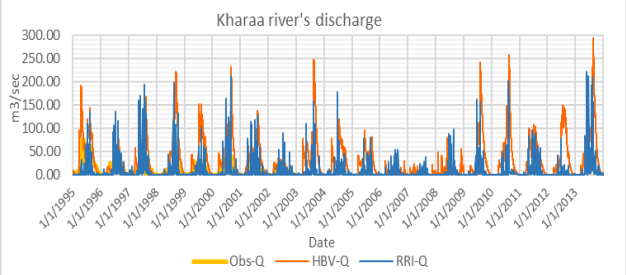

Figure 2. Observed and simulated discharge using RRI and HBV model.

Model parameters were manually calibrated by focusing on the Kharaa river's daily discharge. Table 1 shows the calibrated parameters for mountain and plain areas. The sensitivity analysis covers the period of 2005-2013. However, due to the reliability of observed discharges, we focus here on the entire period 1995-2013 for the model evaluation.

We used three metrics including Nash-Sutcliffe efficiency (NSE), coefficient of determination (r^2) and relative volume error (VE) to evaluate the model performance (see Appendix). The evaluated statistics of the RRI model were NSE = 0.80, r^2 =0.89, VE = 0.04 in the calibration period and NSE = 0.89, r^2 = 0.89, VE = 0.01 in the validation period. In the HBV model, NSE was 0.5-0.7 during the calibration period (1995-2005) (Munkhtsetseg, 2008). When runoff was evaluated using HBV model in the validation period (2005-2013), NSE was 0.5-0.8 (Amarbayasgalan et al., 2015).

The entire river basin was subdivided into two regions: mountain and plain areas. A type S-S (surface + subsurface) model is applied to the mountain area with parameters related to soil depth d_a and d_m, lateral saturated hydraulic conductivity k_a and an exponent parameter β related to unsaturated hydraulic conductivity. A type S-I (surface + infiltration) model is applied to the plain area with the G-A model. Their parameters include vertical saturated hydraulic conductivity k_v, porosity φ and wetting front soil suction head S_f, whose values are referred to by Raws et al. (1992). The parameters n and n_{river} are Manning's roughness coefficients for land surface and river channels. Details of the parameters used in the RRI model were shown in Table 1.

Table 1. The RRI model parameter setting.

	Parameters	Mountains	Plains
n	($m^{-1/3}s$)	0.35	0.35
d_a	(m)	3.0	-
d_m	(m)	1.0	
K_a	(ms^{-1})	1.6	-
β	(-)	4.0	-
k_v	(cmh^{-1})	0.0	0.06
φ		3.8	0.471
S_f		3.1	0.273
F_{limit}	(m)	-	0.4
n_{river}	($m^{-1/3}s$)	0.03	0.03

Summary and Conclusions

In this study, we have estimated runoff of Kharaa river using RRI model. We have split the entire period (1995–2013) into a calibration period (1995–2005) and validation period (2005–2013). We have used three statistics including Nash-Sutcliffe efficiency (NSE), coefficient of determination (r^2) and relative volume error (VE) to evaluate the model performance (see Appendix). The evaluation statistics results of RRI model were NSE = 0.80, r^2 =0.89, VE = 0.04 in the calibration period and NSE = 0.89, r^2 = 0.89, VE = 0.01 in the validation period. For the HBV model, NSE was 0.5–0.8. In order to quantify the hydrologic sensitivity, this study simulated long term rainfall-runoff trends for the entire river basin. (14,530 km^2) using RRI and HBV models. We could compare runoff estimated from RRI and HBV models. Our analysis also suggested that estimated runoff of from RRI model in this basin had the highest correlation with the observed runoff.

Acknowledgments

This study was supported by the Asian Satellite Campuses Institute, Nagoya University, Japan. We also appreciate Institute of Meteorology and Hydrology, Mongolia.

References

Amarbayasgalan Yo et al., 2015. Climate change impact on Kharaa river discharge using HBV hydrological model, (Master's thesis).

Cash, J.R. and Karp, A. H. A variable order Runge-Kutta method for initial value problems with rapidly varying right- hand sides, ACM T. Math. Software, 16, 201-222, 1990.

Chow, V.T., 1973. Hydrodynamic modelling of two-dimensional watershed flow. Journal of the Hydraulics Division of the American Society of Civil Engineers, 2023-2040.

Dooge. J. C. I et al., Sensitivity of runoff to climate change: a Hortonian approach, B. Am. Meteorol. Soc., 73, 2013-2024, 1992.

Hiyama, T. et al., 2016. Recent interdecadal changes in the interannual variability of precipitation and atmospheric circulation over northern Eurasia, Environmental Research Letters. Environ. Res. Lett. 11 (2016) 065001, doi: 10.1088/1748-9326/11/6/065001.

Iwasa, Y. and Inoue, K. Mathematical simulation of channel and overland flood flows in view of flood disaster engineering, Journal of Natural Disaster Science, 4, 1-30, 1982.

Lehner, B., Verdin, K., and Jarvis, A. New global hydrography derived from spaceborne elevation data, EOS T. Am. Goephys. Un., 89, 93-94, 2008.

MARCC, (2014) Mongolia Second Assessment Report on Climate Change 2014. Ministry of Environment and Green Development of Mongolia.

Masutani, K., Akai, K., and Magome, J. A new scaling algorithm of gridded river networks, Journal of Japan Society of Hydrology and Water Resources, 19, 139-150, 2006.

Munkhtsetseg Z., 2008. Hydrological model (HBV) in the Kharaa river basin, (Master's thesis).

Raws W. J., Ahuja L. R., Brakensiek D. L. and Shirmohammadi A. (1992). Infiltration and soil water movement, Handbook of Hydrology (ed), New York.

Sayama, T. et al., 2015. Hydrologic sensitivity of flood runoff and inundation: 2011 Thailand floods in the Chao Phraya River basin, Nat. Hazards Earth Syst. Sci., 15, 1617-1630, 2015, doi: 10.5194/nhess-15-1617/2015.

Sayama, T. et al., 2012. Rainfall-Runoff-inundation analysis of the 2010 Pakistan flood in the Kabul River basin, Hydrological Sciences Journal. Nat. Hazards Earth Syst. Sci., 15, 1617-1630, 2015, doi: 10.5194/nhess-15-1617/2015.

Takuma Takasao, Michiharu Shiiba, Yutaka Ichikawa., 1995. A Runoff simulation with structural Hydrological Modelling system. Proceedings of Hydraulic Engineering, volume 39, pages 141-146.

Appendix

To evaluate the model performance with respect to simulated discharge against observed discharge, we used the following three metrics.

1) Nash-Sutcliffe efficiency (NSE):

$$NSE = 1 - \frac{\sum(Q_{sim}\ (t) - Q_{obs}(t))^2}{\sum(Q_{obs}\ (t) - \overline{Q_{obs}}(t))^2}$$

2) Coefficient of determination (squared correlation coefficient) (r^2):

$$r^2 = \frac{\sum((Q_{sim}\ (t) - \overline{Q_{sim}})(Q_{obs}\ (t) - \overline{Q_{obs}}))^2}{(Q_{sim}\ (t) - \overline{Q_{sim}})^2 \sum(Q_{obs}\ (t) - \overline{Q_{obs}})^2}$$

3) Relative volume error (VE):

$$VE = \frac{\sum(Q_{sim}\ (t) - Q_{obs}(t)}{\sum Q_{obs}(t)}$$

where Q_{sim} (t) and Q_{obs} (t) are simulated and observed discharge at time step t and Q_{obs} is average observed discharge in time.

NSE is a composite measure of bias and random errors; the value is 1 for perfect prediction and 0 if the prediction is no better than the average, and negative for worse than the average. r^2 is a measure of random errors after scaling with a linear relationship; the value is 1 for perfect positive association and 0 if there is no linear correlation. VE is a measure of relative volume errors and the value is 0 for perfect volume agreement while positive (negative) means over (under-) estimation of volume by a model.